Article

Electro-oxidation of Carbon Monoxide on Well-Ordered Pt(111)/Sn Surface Alloys

Brian E. Hayden, Michael E. Rendall, and Oliver South

J. Am. Chem. Soc., **2003**, 125 (25), 7738-7742• DOI: 10.1021/ja0214781 • Publication Date (Web): 28 May 2003

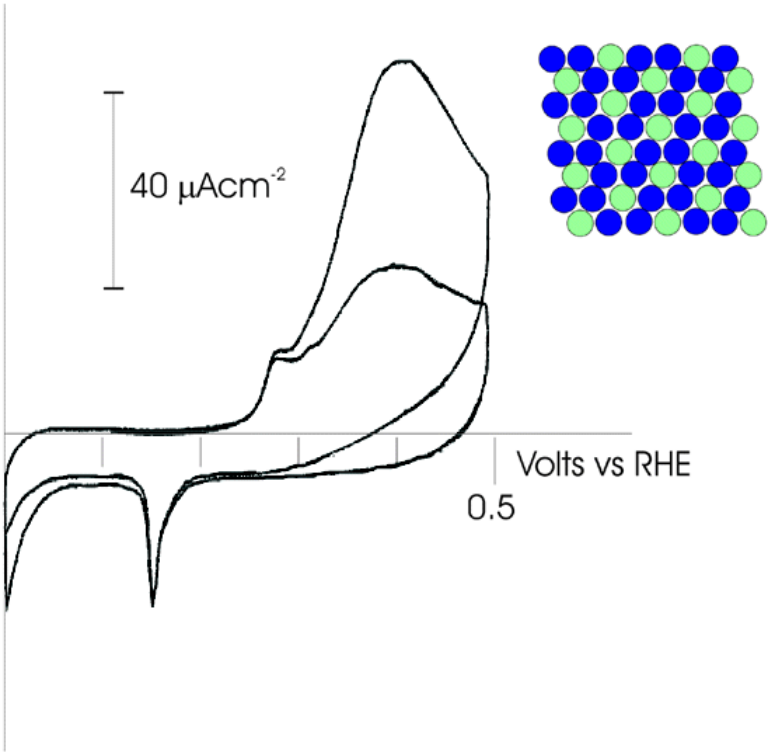

More About This Article

Additional resources and features associated with this article are available within the HTML version:

- Supporting Information
- Links to the 7 articles that cite this article, as of the time of this article download
- Access to high resolution figures
- Links to articles and content related to this article
- Copyright permission to reproduce figures and/or text from this article

J|A|C|S
ARTICLES
Published on Web 05/28/2003

Electro-oxidation of Carbon Monoxide on Well-Ordered Pt(111)/Sn Surface Alloys

Brian E. Hayden,* Michael E. Rendall, and Oliver South

Contribution from the Department of Chemistry, The University of Southampton, Southampton SO17 1BJ, U.K.

Received December 27, 2002; E-mail: beh@soton.ac.uk

Abstract: The electro-oxidation of CO on model platinum−tin alloy catalysts has been studied by ex-situ electrochemical measurements following the preparation of the Pt(111)/Sn(2×2) and Pt(111)/Sn($\sqrt{3}\times\sqrt{3}$)-*R*30° surfaces. A surface redox couple, which is associated with the adsorption/desorption of hydroxide on the Sn sites, is observed at 0.28 V_{RHE}/0.15 V_{RHE} in H_2SO_4 electrolyte on both surfaces. Evidence that it is associated with the adsorption of OH comes from ex-situ photoemission measurements, which indicate that the Sn atoms are in a metallic state at potentials below 0.15 V_{RHE} and an oxidized state at potentials above 0.28 V_{RHE}. Specific adsorption of sulfate anions is not associated with the surface process since there is no evidence from photoemission of sulfate adsorption, and the same surface couple is observed in the $HClO_4$ electrolyte. CO is adsorbed from solution at 300 K, with saturation coverages of 0.37 ± 0.05 and 0.2 ± 0.05 ML, respectively. The adsorbed CO is oxidatively stripped at the potential coincident with the adsorption of hydroxide on the tin sites, viz., 0.28 V_{RHE}. This strong promotional effect is unambiguously associated with the bifunctional mechanism. The Sn-induced activation of water, and promotion of CO electro-oxidation, is sustained as long as the alloy structure remains intact, in the potential range below 0.5 V_{RHE}. The results are discussed in the light of the requirements for CO-tolerant platinum-based electrodes in hydrogen fuel cell anode catalysts and catalysts for direct methanol electro-oxidation.

Introduction

The promotion of CO electro-oxidation at low overpotentials on platinum surfaces can provide the CO tolerance required of anode catalysts in reformate fuelled PEM fuel cells.[1] Such promoted surfaces may also provide active catalysts for the direct oxidation of methanol in direct methanol PEM[2] fuel cells, since CO is a potentially poisoning intermediate in the surface reaction. The alloying of a second, or even third, metal component in platinum has been the favored method of providing CO-tolerant anode catalysts, and to date the most active catalytic system for both applications is the Pt/Ru alloy.[3] The mechanism by which the Ru component of the alloy affords CO tolerance has been investigated in a number of studies of CO oxidation at well-characterized surfaces of Pt/Ru bulk polycrystalline alloys[4−6] and ruthenium-modified single-crystal platinum surfaces.[7−12] The adsorption and reaction of CO on Pt/Ru has also been the subject of kinetic modeling[13,14] and ab initio calculation.[15−17] The results suggest that the promotion of CO electro-oxidation through the activation of water by the ruthenium component in the surface (to provide the oxidant in a bifunctional mechanism) and an electronic effect of Ru on Pt ensuring lower mean coverages of CO are two possible mechanisms by which CO tolerance is afforded.

The Pt/Sn alloy system has been suggested to be a potential alternative CO-tolerant PEM, and DMFC, anode electrocatalysts, since it was suggested to exhibit superior characteristics even to the Pt/Ru alloy for methanol oxidation.[18−20] The mechanism by which the activity was induced by Sn was suggested to be a result of an electronic (ligand) effect of Sn on CO, promoting its oxidation.[18,19] Since then, the promoting mechanism has been the subject of considerable debate (see ref 21 and references

(1) McNicol, B. D.; Williams, K. R. *J. Power Sources* **2001**, *100*, 47−59.
(2) Paola Costamagna, S. S. *J. Power Sources* **2001**, *102*, 242−252.
(3) Wasmus, S.; Kuver, A. *J. Electroanal. Chem.* **1999**, *461*, 14−31.
(4) Gasteiger, H. A.; Markovic, N.; Ross, P. N.; Cairns, E. J. *J. Phys. Chem.* **1994**, *98*, 617.
(5) Gasteiger, H. A.; Markovic, N. M.; Ross, P. N. *J. Phys. Chem.* **1995**, *99*, 8290−8301.
(6) Gasteiger, H. A.; Markovic, N. M.; Ross, P. N. *J. Phys. Chem.* **1995**, *99*, 16757−16767.
(7) Davies, J. C.; Hayden, B. E.; Pegg, D. J. *Electrochim. Acta* **1998**, *44*, 1181−1190.
(8) Davies, J. C.; Hayden, B. E.; Pegg, D. J. *Surf. Sci.* **2000**, *467*, 118−130.
(9) Davies, J. C.; Hayden, B. E.; Pegg, D. J.; Rendall, M. E. *Surf. Sci.* **2002**, *496*, 110−120.
(10) Waszczuk, P. ; Wieckowski, A.; Lu, C.; Rice, C.; Masel R. I. *Electrochim. Acta* **2002**, *47*, 3637−3652.
(11) Hayden, B. E. In *Catalysis and Electrocatalysis at Nanoparticle Surfaces*; Wieckowski, A., Ed.; Marcell Dekker: New York, 2002.
(12) Friedrich, K. A.; Dickinson, J.; Stimming, U. *J. Electroanal. Chem.* **2002**, *524−525*, 261−272.
(13) Koper, M. T. M.; Lukkien, J. J.; Jansen, A. P. J.; van Santen, R. A. *J. Phys. Chem. B* **1999**, *103*, 5522−5529.
(14) Koper, M. T. M.; Lebedeva, N. P.; Hermse, C. G. M. *J. Chem. Soc., Faraday Discuss.* **2002**, *121*, 301−311.
(15) Christoffersen, E.; Liu, P.; Ruban, A.; Skriver, H. L.; Norskov, J. K. *J. Catal.* **2001**, *199*, 123−131.
(16) T. E. Shubina; Koper, M. T. M. *Electrochim. Acta* **2002**, *47*, 3621−3628.
(17) Koper, M. T. M.; Shubina, T. E.; van Santen, R. A. *J. Phys. Chem. B* **2002**, *106*, 686−692.
(18) Janssen, M. M. P.; Moolhuysen, J. *Electrochim. Acta* **1976**, *21*, 861−868.
(19) Janssen, M. M. P.; Moolhuysen, J. *J. Catal.* **1977**, *46*, 289−296.
(20) Rahim, M. A. A.; Khalil, M. W.; Hassan, H. B. *J. Appl. Electrochem. Cairo Univ, Fac. Sci., Dept. Chem., Giza, Egypt* **2000**, *30*, 1151−1155.
(21) Grantscharova-Anderson, E.; Anderson, A. B. *Electrochim. Acta* **1999**, *44*, 4543.

10.1021/ja0214781 CCC: $25.00

therein) and is complicated by the possible influence of Sn on the dehydrogenation reaction in addition to the removal of the CO intermediate. A series of experiments of well-characterized surfaces of Sn-modified Pt, Pt/Sn, single-crystal surfaces provide a considerable insight regarding the influence of Sn in CO[22−25] and methanol[23,26] oxidation. It was found that methanol oxidation was not promoted by Sn on the surface, but could be promoted by a solution phase redox couple involving Sn. It was also concluded that steady state CO electro-oxidation was indeed promoted by Sn at the surface. However, the adsorption and stripping experiments suggested that not all CO was oxidized at low potential, and it was concluded that it must be the remaining CO that dominated the kinetics of methanol oxidation.

Recently, the promotion of CO electro-oxidation by islands of UPD Sn on Pt(111) was again explained by an electronic perturbation of the CO,[27] and indeed a slight weakening of the Pt−CO bond is also evidenced in TPD measurements made on the ordered Pt(111)/Sn alloy surfaces.[28] The originally proposed ligand effect[18,19] was partly substantiated by the absence of a surface redox couple that could account for CO electro-oxidation at low potentials. The redox couple, associated with UPD[29] and spontaneously deposited[30] Sn, is observed at 0.6 V_{RHE}/0.56 V_{RHE} on Pt(111). Nevertheless it is suggested[31] that a surface Sn^{2+} species is active in the electro-oxidation CO and intermediates associated with the oxidation of methanol and formic acid.

We have employed metal vapor deposition (MVD) of Sn on the Pt(111) surface to produce two well-ordered surface alloys of Pt/Sn,[28,32,33] Pt(111)/Sn(2×2) with $\theta_{Sn} = 0.25$ and Pt(111)/Sn($\sqrt{3}\times\sqrt{3}$)*R*30° with $\theta_{Sn} = 0.33$. Figure 1 shows the LEED patterns measured for the two alloys together with the reciprocal space structure and the corresponding real space structures. These well-defined model Pt/Sn alloy surfaces have been used to investigate the surface redox behavior of Sn and specifically its ability to activate water. We show that the activation of water to produce adsorbed hydroxide takes place at very low overpotential and is quite distinct from the Sn^{2+}/Sn^{4+} couple, which gives rise to oxidative dissolution of the Sn. Importantly we also show unambiguously that the CO electro-oxidation on such surfaces takes place coincidentally with the activation of water by the Sn site. This provides direct evidence that promotion takes place by provision of the oxidant at low overpotential through a bifunctional mechanism.

Experimental Section

The UHV/electrochemical transfer system for ex-situ electrochemical measurements is described in detail elsewhere.[34] The MVD Sn source was a resistively heated tantalum boat Knudsen cell containing pure tin wire (99.99+%, Goodfellow) with the temperature of the source measured with a Chromel-Alumel thermocouple. Tin was deposited at a boat temperature of 800 K and a deposition rate of ca. 0.05 ML min^{-1}, as monitored by in-situ X-ray photoelectron spectroscopy applying the appropriate sensitivity factors.[35] The tin was incorporated into the surface to form the alloy phases by flash annealing the platinum crystal to 900 K. The tin surface coverage was also monitored by low-energy ion scattering spectroscopy (LEISS), and the formation of the ordered overlayer by low-energy electron diffraction (LEED). Electrochemistry was performed using a glass cell, after raising the pressure of the antechamber, to which the sample was transferred, to atmospheric pressure of oxygen-free argon. The electrolyte was 0.5 M H_2SO_4 or 0.5 M $HClO_4$, and a Pd/H_2 couple was used as reference electrode. All solutions were made using ultrapure (Millipure) water (conductivity > 18 $M\Omega^{-1}$ cm^{-2}).

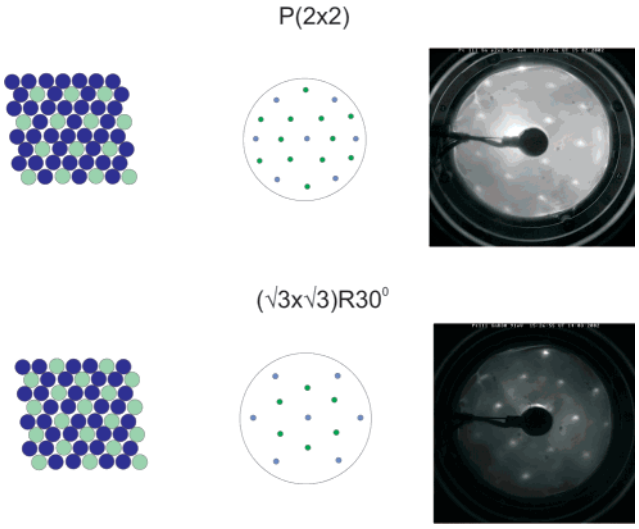

Figure 1. LEED patterns (together with the reciprocal space structures) obtained for the Pt(111)/Sn(2×2) and Pt(111)/Sn($\sqrt{3}\times\sqrt{3}$)*R*30° surface alloys. The beam energies were 57 and 91 eV, respectively. A real space representation of the surfaces is also shown, with the incorporated Sn atoms shown as the lighter spheres.

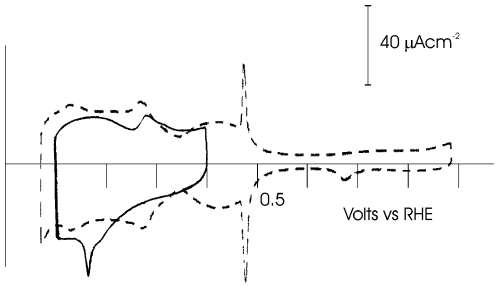

Figure 2. Cyclic volammograms of Pt(111) (dashed line) and Pt(111)/Sn($\sqrt{3}\times\sqrt{3}$)*R*30° (solid line) surfaces in 0.5 M H_2SO_4. The scan rate was 100 mV s^{-1}.

Results and Discussion

Surface Redox Behavior of the Pt/Sn Alloy. Figure 2 shows the cyclic voltammetry (CV) of the Pt(111) surface (broken line) and the Pt(111)/Sn($\sqrt{3}\times\sqrt{3}$)*R*30° alloy surface (solid line), both in 0.5 M H_2SO_4 electrolyte, measured at a sweep rate of 100 mV s^{-1}. The Pt(111) "butterfly" structure is that expected for a clean, well-ordered surface, exhibiting the reversible hydrogen and sulfate adsorption structure, the sharp long-range ordering

(22) Markovic, N. M.; Widelov, A.; Ross, P. N.; Monteiro, O. R.; Brown, I. G. *Catal. Lett.* **1997**, *43*, 161−166.
(23) Wang, K.; Gasteiger, H. A.; Markovic, N. M.; Ross, P. N. *Electrochim. Acta* **1996**, *41*, 2587−2593.
(24) Gasteiger, H. A.; Markovic, N. M.; Ross, P. N. *Catal. Lett.* **1996**, *36*, 1−8.
(25) Gasteiger, H. A.; Markovic, N. M.; Ross, P. N. *J. Phys. Chem.* **1995**, *99*, 8945−8949.
(26) Haner, A. N.; Ross, P. N. *J. Phys. Chem.* **1991**, *95*, 3740−3746.
(27) Xiao, X. Y.; Baltruschat, H. *Phys. Chem. Chem. Phys* **2002**, *4*, 4044−4050.
(28) Paffett, M. T.; Gebhard, S. C.; Windham, R. G.; Koel, B. E. *J. Phys. Chem.* **1990**, *94*, 6831−6839.
(29) Massong, H.; Wang, H.; Samjeske, G.; Baltruschat, H. *Electrochim. Acta* **2000**, *46*, 701−707.
(30) Campbell, S. A.; Parsons, R. *J. Chem. Soc., Faraday Trans.* **1992**, *88*, 833.
(31) Norton Haner, A.; Ross, P. N. *J. Phys. Chem.* **1991**, *95*, 3740−3746.
(32) Paffett, M. T.; Windham, R. G. *Surf. Sci.* **1989**, *208*, 34−54.
(33) Xu, C.; Koel, B. E.; Paffett, M. T. *Langmuir* **1994**, *10*, 166−171.
(34) Hayden, B. E.; Murray, A. J.; Parsons, R.; Pegg, D. J. *J. Electroanal. Chem.* **1996**, *409*, 51−63.
(35) Briggs, D.; Seah, M. *Practical Surface Analysis by Auger and X-ray Photoelectron Spectroscopy*; John Wiley & Sons Ltd.: Chichester, 1983.

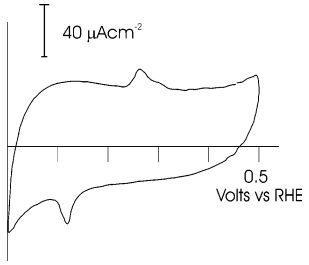

Figure 3. Cyclic volammogram of the Pt(111)/Sn($\sqrt{3}\times\sqrt{3}$)*R*30° (solid line) surface in 0.5 M $HClO_4$. The scan rate was 100 mV s^{-1}.

peaks at 0.48 V_{RHE}, and the sulfate/bisulfate structure above 0.6 V_{RHE}.

In the case of the superimposed voltammetry of the alloy surface, the CV shown was the first obtained following preparation in UHV and transfer to the electrochemical cell: The observed structure remained unchanged as long as the potential was not raised above ca. 0.5 V_{RHE}. The hydrogen UPD structure in the potential range of the measurement (e.g., the reversible peaks at ca. 0.26 V_{RHE}) of the Pt(111) surface is largely destroyed by the presence of Sn, although there remains an underlying pseudo-capacitance which may be associated with hydrogen adsorption. The volammogram of the alloy surface exhibits small and relatively sharp peaks superimposed on the broadened double layer current in the anodic and cathodic scans at 0.28 V_{RHE}/0.15 V_{RHE}, respectively. Current densities are given, but it should be noted that there is an absolute error of ± 10 μA cm^{-2} since it was difficult to define the meniscus contact area on the face of the crystal since the incorporation of the Sn resulted in strong wetting of the surface on contact. The peaks in the anodic and cathodic scans at 0.28 V_{RHE}/0.15 V_{RHE} are associated with a surface redox couple involving the adsorption and desorption of OH at the platinum sites. Evidence that it is associated with the reversible oxidation of the Sn atoms is given below in photoemission experiments. The possibility that the observed peaks in the voltammetry were associated with the specific adsorption of sulfate anions was considered and rejected on a number of pieces of evidence. First, no sulfate adsorption is observed in ex-situ photoemission experiments following transfer of the surface back to UHV after breaking contact at 0.4 V_{RHE}. It will also be shown, below, that the underlying structure of the anodic peak remains in the presence of adsorbed CO. Most importantly, the experiment was also carried out on the Pt(111)/Sn($\sqrt{3}\times\sqrt{3}$)*R*30° alloy surface in $HClO_4$ electrolyte, and the results are shown in Figure 3. The same structure in the voltammetry, at 0.27 V_{RHE}/0.12 V_{RHE}, is observed. The alloy-induced peaks in the voltammetry carried out in H_2SO_4 electrolyte are clearly not associated with sulfate adsorption.

Figure 4 shows the CV of the two surface alloy structures Pt(111)/Sn(2×2) and Pt(111)/Sn($\sqrt{3}\times\sqrt{3}$)*R*30°, measured in H_2SO_4 electrolyte at a sweep rate of 100 mV s^{-1}. The associated LEED patterns and the real space structures for the alloys are also shown in Figure 1. LEED revealed that the ordered alloy was formed over the complete Pt(111) surface in both cases. The CV shown was the first measured on the transferred surfaces and remained unaltered in further scans as long as the potential was not raised above ca. 0.5 V_{RHE}. Both surfaces exhibit the small and relatively sharp peaks superimposed on a broad double layer current in the anodic and cathodic scans at 0.28 V_{RHE}/

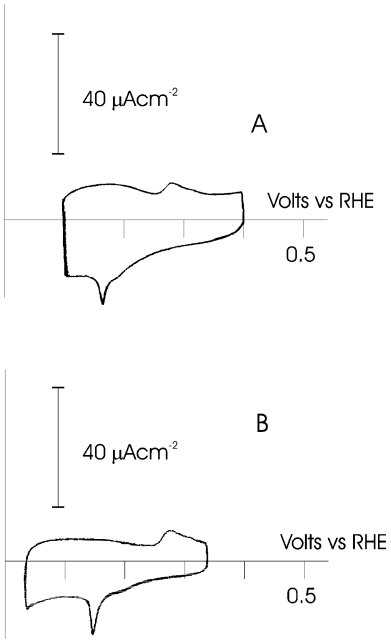

Figure 4. Cyclic volammograms of Pt(111)/Sn(2×2) (A) and Pt(111)/Sn-($\sqrt{3}\times\sqrt{3}$)*R*30° (B) surfaces in 0.5 M H_2SO_4. The scan rate was 100 mV s^{-1}.

0.15 V_{RHE}, respectively, which we associate with OH adsorption/desorption. The peaks are found at the same potential for the two alloy surfaces. The common potential for the couple is understandable assuming it is the immediate surroundings of the Sn atoms that dominated the electronic response (Sn atoms are surrounded by platinum atoms in both structures), and next nearest Sn atoms have little or no influence on the surface redox behavior. This surface redox couple is quite different from the Sn^{2+}/Sn^{4+} couple observed from Sn deposition from solution at 0.62 V_{RHE}/0.42 V_{RHE}, which is characteristic of bulk Sn surfaces or clusters on platinum.[30]

To confirm the change in oxidation state of the Sn associated with hydroxide adsorption, meniscus contact between the crystal and the electrolyte was broken at two potentials, 0.1 V_{RHE} and 0.4 V_{RHE}, above and below the potentials associated with the OH adsorption process. This experiment was carried out on the Pt(111)/Sn($\sqrt{3}\times\sqrt{3}$)*R*30° alloy surface. In each case, the electrochemical antechamber was evacuated and the crystal immediately transferred back to the UHV chamber in order to carry out X-ray photoelectron spectroscopy. The results in the form of the Sn(3d) doublet are shown in Figure 5. Figure 5A follows emersion at 0.1 V_{RHE} and shows that the Sn atoms remain in the same metallic state as that observed on preparation of the alloy in UHV. Note that the surface had been previously cycled to 0.4 V_{RHE}. Figure 5B shows the same photoemission spectrum measured following emersion at 0.4 V_{RHE}. It is evident that the Sn now exhibits two oxidation state, Sn^0 ($Sn(3d^{3/2})$ = 489 eV) and ca. Sn^{2+} ($Sn(3d^{3/2})$ = 492 eV), using results of core level shifts of a variety of Sn compounds[35] to establish the Sn^{2+} oxidation state. Note that this does not indicate necessarily that the "in-situ" oxidation state of Sn following OH adsorption is around Sn^{2+}, since chemical reaction following transfer may result in some associative water formation. However it does unambiguously indicate that the Sn atoms are in an oxidized state at potentials above the anodic peak at 0.28 V_{RHE} and that this state does not correspond to Sn^{4+}. One may

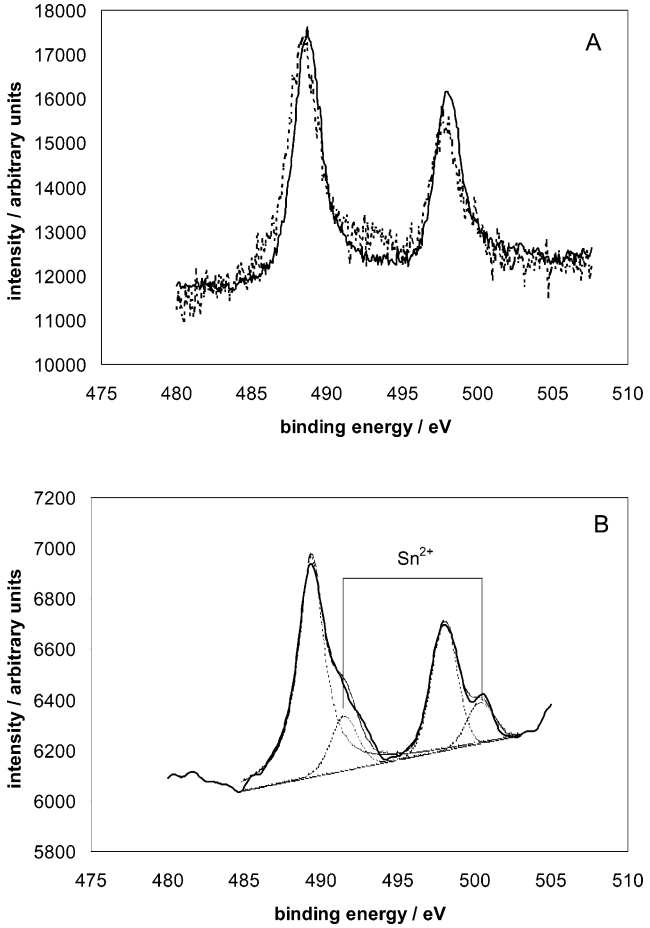

Figure 5. X-ray photoelectron spectrum (Sn(3d) region) of the Pt(111)/Sn($\sqrt{3}\times\sqrt{3}$)*R*30°alloy surface (A) before transfer to the electrochemical cell (dotted line) and after emersion at 0.1 V_{RHE} following several cycles to 0.4 V_{RHE} and transferring the surface back into the UHV chamber. (B) Photoemission spectrum following emersion at 0.4 V_{RHE}. Following background subtraction, the measured spectrum (solid line) has been deconvoluted into the contributions of the Sn^0 and Sn^{2+} components (dotted lines), and the sum of these is shown (dashed line) for comparison with the original spectrum.

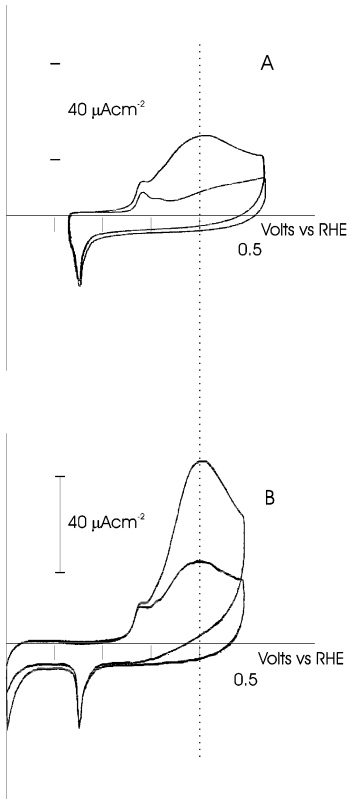

Figure 6. CO stripping volammograms of saturated overlayers of CO on Pt(111)/Sn(2×2) (A) and Pt(111)/Sn($\sqrt{3}\times\sqrt{3}$)*R*30° (B) surfaces in 0.5 M H_2SO_4. The scan rate was 100 mV s^{-1}. CO was adsorbed from a CO-saturated 0.5 M H_2SO_4 solution under potential control (0.05 V_{RHE}), and the CO stripped in CO-free electrolyte.

have expected all Sn atoms in the top surface layer to have the oxidized state. However the XPS measurement includes part of the Pt(111) surface that has not made contact with the electrolyte. In addition, we find that a Sn concentration in the top four layers (measured at these kinetic energies in in XPS) is required in order to establish a well-formed ordered surface alloy structure. The unoxidized Sn therefore is associated with the area of the surface outside the meniscus contact area, and a component incorporated below the top surface layer.

CO Electro-oxidation on the Pt/Sn Alloy. The Pt(111)-Sn-(2×2) and Pt(111)/Sn($\sqrt{3}\times\sqrt{3}$)*R*30° surfaces were transferred from UHV and exposed to CO contained in a CO-saturated 0.5 M H_2SO_4 solution at 0.05 V_{RHE}. The surface was exposed to the CO for sufficient time (5 min) to ensure that the surface (exclusively the Pt sites[25]) was saturated. The electrolyte was then replaced with CO-free 0.5 M H_2SO_4, and CO stripping voltammetry carried out (Figure 6) in the potential range corresponding to the Sn alloy redox behavior (Figure 4) and up to 0.5 V_{RHE}. The upper potential limit was chosen because of the further oxidation of Sn at higher potentials leading to oxidative dissolution of the Sn component. The overpotential for CO electro-oxidation on Pt(111) under these conditions is 0.8 V_{RHE}.[9] The first scan of the CV shows a broad oxidation peak at 0.4 V_{RHE}, with an onset coincident with the Sn oxidation peak at 0.28 V_{RHE}. This corresponds to the oxidation of the adsorbed CO. The second scan shows that nearly the entire CO overlayer on the surface was oxidized in the first sweep. Complete stripping was only hindered by the restriction of the upper potential limit. The coverages of CO on the Pt(111)/Sn-(2×2) and Pt(111)/Sn($\sqrt{3}\times\sqrt{3}$)*R*30° surfaces, estimated from the associated stripping charges, were 0.37 ± 0.05 and 0.2 ± 0.05 ML. This is about half the saturation coverages observed for CO adsorption at low temperature on the same alloy surfaces in UHV and corresponds to about one CO molecule per two Pt atoms in the surface layer for both structures.[28] One may have expected that dosing at room temperature in the electrolyte at higher effective pressures may have given coverages similar to those observed at low temperature, as found for Pt(111). However, alloying the Pt(111) surface with Sn results in a significant reduction in the CO desorption temperature, and this may result in lower saturation coverages at room temperature on the Pt(111)/Sn(2×2) and Pt(111)/Sn($\sqrt{3}\times\sqrt{3}$)*R*30° surfaces. Note that there is an underlying increase in current (Figures 3, 4, and 6) above 0.4 V_{RHE} that is observed in the absence of CO. This we associate with the onset of further oxidation of Sn in the alloy (to Sn^{4+}), which under these conditions eventually results in Sn dissolution and destruction of the alloy above 0.5 V_{RHE}. In scans to higher potential (not shown), which quickly destroy the ordered alloy surface and the associated surface redox behavior, this further oxidation leads to a small broad peak in the anodic scan at ca. 0.8 V_{RHE}, and such

experiments indicate that on CO-covered surfaces no CO stripping is observed at higher potentials.

The coincident onset of the CO electro-oxidation with the Sn oxidation (Figure 6) on the alloy surface is the first time the operation of the bifunctional mechanism has been observed unambiguously. Such a mechanism is generally accepted for the Pt/Ru system;[36−38] however there is no corresponding surface redox process associated with the provision of the oxidant by the ruthenium that can be identified on the CO-free surface. It appears that the charge associated with the activation of the water to provide the surface-adsorbed oxidant is generally very small, as evidenced by the very small currents associated with the process on the Pt(111)/Sn alloy surfaces.

Very recent X-ray measurements of the $Pt_3Sn(111)/(2\times2)$ surface structure[39] reveal significant extension of the Pt−Sn bond distance and a relaxation of the Pt interlayer spacing, in the surface of the potential region $0.5 < V_{RHE} < 0.55$. This potential region includes the potentials at which we are suggesting that OH adsorption takes place on the surface alloy structures. The large changes observed in the interlayer spacings are consistent with the adsorption of OH, but is not clear why the effective rumpling takes place over a relatively wide potential range. We note that the sharp redox behavior observed in these studies is not observed in the voltammetry of the $Pt_3Sn(111)/(2\times2)$ surface. On the other hand, the reversible broad structure observed at 0.35 V_{RHE}, correlated with (bi)sulfate adsorption,[39] is not observed on the surface alloy structures (Figure 3). We can only suggest that this difference may be associated with either intrinsic differences between the behavior of the surface generated at the termination of the bulk alloy and the surface alloy or the extent of surface order.

This observed overpotential for CO electro-oxidation (the peak potential) is considerably lower than bare platinum (by 0.4 V) and ruthenium-modified Pt(111) (by 0.2 V),[9,40] suggesting that well-alloyed Pt/Sn catalysts may provide excellent CO-tolerant electrodes and may have activity for methanol oxidation. The result is consistent with the observation that steady state CO oxidation is strongly promoted by Pt/Sn.[24,41] We observe, however, that on these ordered alloy surfaces, complete stripping of the CO on the small Pt ensembles takes place at the low overpotential (Figure 6), and oxidation of adsorbed CO at higher potentials takes place only when the alloyed Sn is oxidatively stripped from the alloy surfaces. It was the presence of a second CO species oxidized at higher potentials that was the explanation[23] for the absence of promotion in methanol oxidation on Pt/Sn alloys.[25]

The potential of the alloy surfaces for CO-tolerant catalysts, or catalysts for methanol oxidation, appears therefore to hinge on the activity of the small platinum ensembles to oxidize hydrogen or methanol. Experiments to establish this are now underway in this laboratory. To ensure activity of such a catalyst, however, once prepared, the alloy structure cannot be exposed to oxidizing environments in the electrolyte corresponding to potentials > ca. 0.5 V_{RHE}.

Conclusions

The electro-oxidation of CO is strongly promoted by Sn on $Pt(111)/Sn(2\times2)Sn$ and $Pt(111)/Sn(\sqrt{3}\times\sqrt{3})R30°$ alloy surfaces. The onset of CO oxidation is coincident with an observed oxidation of the Sn in the alloy surface. This oxidation is associated with the adsorption of hydroxide through the activation of water by Sn. It is evidenced by small peaks in the anodic and cathodic scans of the voltammetry in H_2SO_4 electrolyte on both alloy surfaces at 0.28 V_{RHE}/0.15 V_{RHE} and in $HClO_4$ electrolyte at 0.27 V_{RHE}/0.12 V_{RHE}. The change in the Sn oxidation is substantiated by photoelectron spectroscopy in ex-situ transfer experiments, with immersion at 0.1 V_{RHE} and 0.4 V_{RHE}. This is a clear observation of the promotion of CO electro-oxidation by a bifunctional mechanism. The onset of CO electro-oxidation at such a low overpotential (0.28 V_{RHE}) makes the Pt/Sn alloy system an ideal candidate for CO-tolerant anode catalysts, and for direct methanol oxidation, providing the potential is kept sufficiently low to avoid the destruction of the alloy through oxidative dissolution of the Sn component. It is the activity of the surfaces in the oxidation of hydrogen, and dehydrogenate methanol, that will then determine their suitability as catalyst structures.

Acknowledgment. We wish to acknowledge support for this work from Johnson Matthey Plc and EPSRC under grant number GR/R50639/01.

JA0214781

(36) Watanabe, M.; Motoo, S. *J. Electroanal. Chem.* **1975**, *60*, 267.
(37) Watanabe, M.; Motoo, S. *Electroanal. Chem. Interfacial Electrochem.* **1975**, *60*, 275−283.
(38) Lebedeva, N. P.; Koper, M. T. M.; Feliu, J. M.; van Santen, R. A. *J. Electroanal. Chem.* **2002**, *524*, 242−251.
(39) Stamenkovic, V. R.; Arenz, M.; Lucas, C. A.; Gallagher, M. E.; Ross, P. N.; Markovic, N. M. *J. Am. Chem. Soc.* **2003**, *125*, 2736−2745.
(40) Chrzanowski, W.; Wieckowski, A. *Langmuir* **1997**, *13*, 5974−5978.
(41) Gasteiger, H. A.; Markovic, N. M.; Ross, P. N. **1997**.